Solid State Power Amplifier Combiners for Accelerator Applications

Christopher Fadden
School of Electrical and Computer Engineering
Georgia Institute of Technology
Atlanta, GA, USA

***Abstract*—Two different power combiner simulations are presented. A discussion on the background of transmission lines is given for a coaxial tree power combiner. The successful results of the circuit simulation, as well as the less successful results of the 3D simulation are given. The background of a cavity combiner is discussed, including designs of input and output couplers. The design of two different couplers is presented, a coaxial output coupler and the addition of a cylindrical plate to the end of the coupler. The cylindrical plate gives positive results in terms of loss, but has an unrealistically low efficiency, and therefore more work must be done to confirm its benefits. The end result of this work is a cavity combiner simulation that can be used as the basis for a prototype.**

***Index Terms*—Cavity Combiner, Coaxial Combiner**

I. Introduction

THE very first Radio-Frequency and Microwave circuits were created long before the invention of the transistor. Instead of solid-state switches, vacuum tubes were used to control these circuits. These vacuum tubes operated completely differently from their solid-state cousins, and were expensive, non-dependable devices. Therefore, when the transistor was created as a dependable, predictable alternative, nearly all circuits changed out the tube circuitry. The one place where tubes are still used is in high power amplifiers. Transistors often cannot handle the extremely high power required of these circuits. Individual transistor amplifiers can only output in the kilowatt range of power, while microwave tubes can handle megawatts.

Even though microwave tubes can handle the high power, they also inherit the problems of tube-based circuitry. They are extremely expensive, do not last very long compared to transistors, and a design goal is to phase them out of future projects. In order to get the desired power output from transistors, multiple amplifiers must be used, and then combined to form the final output power. This project is based on analyzing two different types of power amplifier combiners, and finding the best design parameters. This information can then be used to design prototypes and eventually be implemented for use in the Advanced Photon Source.

II. Transmission Line Background

The difference between high-frequency circuit design and its lower-frequency counterpart is the wave-nature of the electric and magnetic fields. In lower frequency electronics, the distance the wave travels is much smaller than a wavelength, and can therefore be ignored. However, in high-frequency circuits, the distances between components are on the order of a wavelength. Therefore, more variables have to be accounted for in order to ensure the circuit behaves as intended. These variables are modeled as transmission lines.

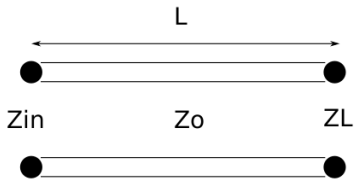

Fig. 1. Ideal Transmission Line

The equations of voltage and current along a transmission line are [1]:

$$V(z) = V_0^+ e^{-j\beta z} + V_0^- e^{j\beta z} \tag{1a}$$

$$I(z) = \frac{V_0^+}{Z_0} e^{-j\beta z} - \frac{V_0^-}{Z_0} e^{j\beta z} \tag{1b}$$

The Z_0 is the intrinsic impedance of the transmission line, and is related to the geometry and material of the line. β is the spatial frequency, $\frac{2\pi}{\lambda}$. The ratio of the reflected wave, V_0^- to the incident wave V_0^+ is extemely important in the design of these circuits. If all the power is to be transmitted to the load, this ratio must be as small as possible. It is related to the impedance of both the line and the load by:

$$\Gamma = \frac{V_0^-}{V_0^+} = \frac{Z_L - Z_0}{Z_L + Z_0} \tag{2}$$

The impedance of the transmission line seen by external components can vary with the length of the line. In order to have the reflection be zero at the beginning of the line, the input impedance of the line must equal the impedance of whatever is connected to it. The input impedance is given by the ratio of voltage to current at the beginning of the line [1].

$$Z_{in} = \frac{V(0)}{I(0)} = Z_0 \frac{(Z_L + Z_0)e^{j\beta z} + (Z_L - Z_0)e^{-j\beta z}}{(Z_L + Z_0)e^{j\beta z} - (Z_L - Z_0)e^{-j\beta z}} \tag{3a}$$

$$Z_{in} = Z_0 \frac{Z_L cos(\beta l) + jZ_0 sin(\beta l)}{Z_0 cos(\beta l) + jZ_L sin(\beta l)} \tag{3b}$$

$$Z_{in} = Z_0 \frac{Z_L + jZ_0 tan(\beta l)}{Z_0 + jZ_L tan(\beta l)} \tag{3c}$$

The impedance seen at the beginning of the line therefore depends on the load, the intrinsic impedance, and the length of the transmission line. This enables matching two different impedances by means of a transmission line transformer. There will be no reflection from either the input or the output, resulting in ideally perfect transmission. Using (3c), there are two special cases often used in microwave design. The first is when the length of the line is equal to $\frac{\lambda}{4}$. Because of the length of the line, this is called a "quarter-wave transformer". It can match any input or output impedance by varying the intrinsic impedance. This works because tangent becomes infinite when βl equals $\frac{\pi}{2}$. Therefore, the intrinsic impedance of a quarter wave transformer, to match loads on both ends, should be:

$$Z_0 = \sqrt{Z_{in} Z_L} \tag{4}$$

The second case that is often used in microwave engineering is using a short circuit stub transmission line. The load impedance of the line is zero. this results in an input impedance of:

$$Z_{in} = jZ_0 tan(\beta l) \tag{5}$$

Because the input impedance for a lossless stub is always imaginary, that means it can only act as a capacitive or inductive part of the circuit. Using stubs is often used to counteract any reactive parts of a load, so that it can be matched using the real impedances of the quarter-wave transformer.

The analysis of microwave circuits is accomplished using two main techniques, scattering parameters and a smith chart. The smith chart is a graphical representation of the impedances in a circuit, and can be used to design the matching circuits to minimize reflections. Scattering parameters use network theory to describe the power flowing into and out of the circuit. The most important scattering parameter is the S_{11}, which represents the reflected power, which is the network representation of (2). Since S_{11} can vary over many orders of magnitude, it is often represented in dB. Therefore, an S_{11} of 0 represents total reflection, and an S_{11} of negative infinity indicates no reflection.

III. Coaxial Combiner Design

The simplest way to combine power is to simply have many coaxial waveguides funnel into a single waveguide, from which the end output power can be extracted. The size of the coaxial waveguide must increase with the increase in power. A common configuration would have the power amplifiers feed 50 Ω lines, and transformers would account for different impedances as less lines were used and the size increased.

The impedance, Z_0, of a coaxial waveguide is given by:

$$Z_0 = \frac{1}{2\pi} \sqrt{\frac{\mu}{\epsilon}} ln\left(\frac{D}{d}\right) \tag{6}$$

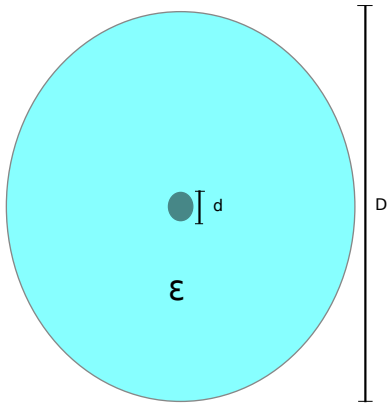

Fig. 2. Coaxial Cable Cross-section

D and d represent the outer and inner diameters of the conductors, and govern the impedance of the line, given a homogeneous dielectric. In order to lessen the dielectric losses of the system, an air dielectric is used for all the waveguides.

IV. Coaxial Combiner Circuit Simulation

The first simulation of the coaxial combiner tree combined the lumped element model of low frequency electronics with the distributed impedance of microwave circuitry. Using CST Microwave Studio, a series of transmission lines were modeled, connected by wires, and terminating at one end with a waveguide port, and ground on the other.

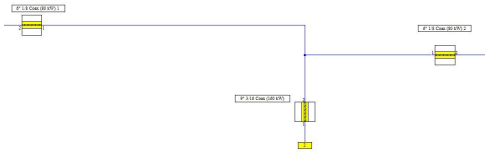

Fig. 3. Coax Tree Circuit Port Termination

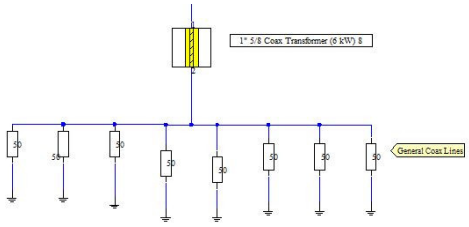

Fig. 4. Coax Tree Circuit Ground Termination

This circuit is based off of design parameters provided in an ESRF report [2]. The outer diameters of the coaxial cables were all provided, and the simulation consisted of finding the correct inner diameter to match the impedance needed. Using (4), (2), and the following formula, the correct impedance can be chosen to prevent reflection:

$$\frac{1}{Z_{parallel}} = \frac{1}{Z_1} + \frac{1}{Z_2} + ... \tag{7}$$

This simulation was a success, determined by the S_{11} measurement having a sharp decline at the specified frequency of interest.

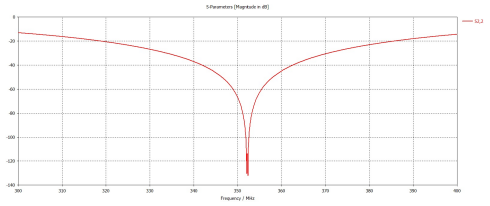

Fig. 5. Reflection Measurement of Coaxial Tree Circuit

V. Coaxial Tree 3-D Simulation

The circuit model of the coaxial tree had results that agreed with the standard one-dimensional treatment of transmission lines. Unfortunately, in a realistic three-dimensional system, the one-dimensional treatment is simply a a starting point, and a 3-D simulation is absolutely necessary. The first change going from circuit to 3-D model was changing the wires. In the circuit, the wires act as perfect connections, simply providing a path from one element to another, with no other effect on the circuit. In the 3-D model, these wires became 50 Ω transmission lines of various sizes. In order to help matching boundary conditions, the outer conductor of the transformers and the wires were the same. This meant that there would be a sharp difference between the inner conductors. The larger inner conductor have a portion that would see an air boundary condition, while the rest would see the rest of the inner conductor. The difference in this boundary condition throws off the hand-calculations based on the 1-D approximation.

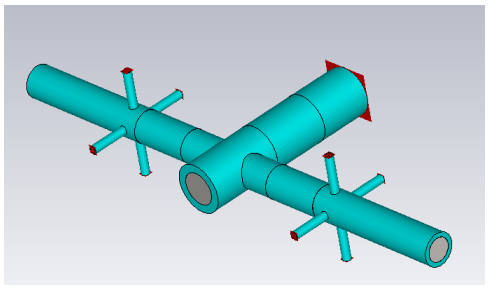

Fig. 6. 3-D Coaxial Tree showing Stub-Matching Elements

In order to match the boundary conditions properly, and get as little reflection as possible, short circuited stubs were added to the design. These stubs, with impedeance given by (5), counter-act any inductance or capacitance that is preventing a matched impedance. Once there is just a real impedance, a match can be made using (4) to match whatever load is there, which in the simulation did not match the 1-D hand calculation. Another complication is the increased computation time for the 3-D simulations. Therefore, only part of the full 128 element circuit was modeled. Because of the difficulty in matching the boundary conditions, the 3-D simulation did not match the results of the circuit simulation.

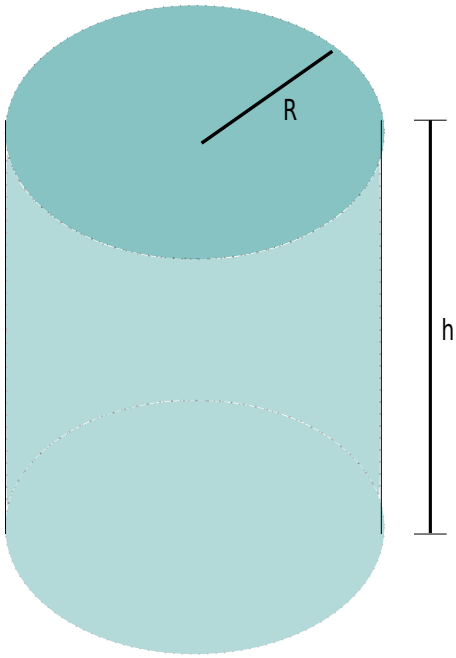

Fig. 7. Cavity Resonator

VI. Cavity Combiner Derivation

The coaxial combiner is a conceptually simple way of combining power. However, coaxial cables have some intrinsic losses that can cause problems at the high power levels of this design. Therefore, a second approach is to use a resonating cavity combiner. This waveguide cavity combiner will have much lower losses than the equivalent coaxial cables, as the only loss is surface currents in the walls, the inputs, and the outputs. The design derivation will assume an ideal cavity, and then modelling software will be used to test non-idealities and provide a basis for a prototype.

The derivation of the cavity resonator will be based on a cavity will perfect electrical conduting walls (PEC), shown in fig. 7. Instead of starting from Maxwell's equations, it makes sense to start from the source-free Helmholtz equations:

$$\nabla^2 E = \frac{1}{v_p^2}\frac{\partial^2 E}{\partial t^2} \tag{8a}$$

$$\nabla^2 H = \frac{1}{v_p^2}\frac{\partial^2 H}{\partial t^2} \tag{8b}$$

When solving these wave equations for a geometry such as a cavity resonator, it makes sense to transform into cylindrical coordinates. When the electric field equaiton is re-written an equation resembling the Bessel equation emerges [3]:

$$\frac{d^2 E_z}{dr^2} + \frac{1}{r}\frac{dE_z}{dr} + \frac{\omega^2}{v_p^2}E_z = 0 \tag{9}$$

Since this equation can be thought of as a Bessel equation, the general solution is given in terms of Bessel functions. By applying the boundary conditions, namely that the electric

field goes to zero at all the walls, the particular solution, and therefore mode frequencies can be found. Since the field distribution depends on Bessel functions, so to do the mode frequencies. The equations for the mode frequencies are given below [1]:

TM

$$f_{m,n,p} = \frac{v_p}{2\pi}\sqrt{\left(\frac{X_{m,n}}{R}\right)^2 + \left(\frac{p\pi}{h}\right)^2} \tag{10a}$$

TE

$$f_{m,n,p} = \frac{v_p}{2\pi}\sqrt{\left(\frac{X'_{m,n}}{R}\right)^2 + \left(\frac{p\pi}{h}\right)^2} \tag{10b}$$

The $X_{m,n}$ signifies the n-th zero of the m-th order Bessel function. $X'_{m,n}$ signifies the n-th zero of the derivative of the m-th order Bessel function. From the boundary conditions enforced, for a TE mode, p must be greater than or equal to 1 [4]. The TM mode has no such constraint, and therefore can have a lower fundamental frequency when p is equal to zero. When designing for this frequency the height does not have any affect, which gives freedom in the spatial construction. For power combining, the TM_{010} mode has been determined to have the best properties for this application [1]. Although the TM modes have no dependence on the hight, the TE modes occur at lower and lower frequencies as the height increases. Therefore, a cavity resembling a "pancake" will achieve the best electromagnetic characteristics, as well as occupying the smallest volume.

Besides choosing a frequency for the cavity, another design consideration is the Q-factor. The Q-factor is related to the bandwidth of the cavity, but more importantly relates the stored potential energy to the power dissipated in the cavity. The formulas for the Q-factor are [3]:

General

$$Q = \frac{2\pi f_0 U}{P} \tag{11a}$$

Cavity

$$Q = \frac{\frac{h}{\delta}}{1 + \frac{h}{R}} \tag{11b}$$

In (11b), the δ is the skin depth of the wall material. Therefore, an air dielectric is both the cheapest and most electromagnetically useful for this application. A key factor relating the coupling of the cavity is the ratio of the Q-factor for the cavity and the external connections to it.

$$\beta = \frac{Q_0}{Q_{ext}} \tag{12}$$

In order to have the most coupling possible, β should be as large as possible. Generally, the Q given by (11a) should depend on frequency. However, because of the specific mode used and the specific geometry of the cavity, the Q of the cavity given by (11b) is independent of frequency. Since Q_0 is set by the geometry, most of the degrees of freedom lie in the external connections inputting and outputting power from the cavity, thereby changing the Q_{ext}.

The validity of a cavity design is characterized by the efficiency of the cavity, as well as the losses present in the cavity, the inputs, and the outputs. The efficiency relates the output power to the input power. The power at each port is given by the surface integral of the Poynting Vector:

$$\vec{S} = \frac{1}{2}\vec{E} \times \vec{H}^* \tag{13}$$

$$P = \int \vec{S} \cdot d\vec{S} \tag{14}$$

The ratio of the sum of the power at all the input ports to the output port gives the efficiency, which ideally should be 100 percent. Besides the efficiency, the losses are an important characteristic of the cavity design. The loss along any surface is given by:

$$Loss = \frac{1}{2}R_s \int \vec{H} \cdot \vec{H}^* d\vec{S} \tag{15}$$

where R_s is the surface resistivity given by:

$$u_s = \sqrt{\frac{\omega\mu}{2\sigma}} \tag{16}$$

ω is the radian frequency, μ is the permeability, and σ is the conductivity.

The efficiency gives how much power did not make it through the output port, and the loss calculations indicate where the rest of the power went. The loss could be measured along the surface of the cavity, the inputs, and the outputs.

VII. Input Coupler Design

The main field excited in the cavity will be the TM_{010} mode. Therefore, the input couplers are designed to provide power using the magnetic field. For this reason, metal loops are used as the input couplers.

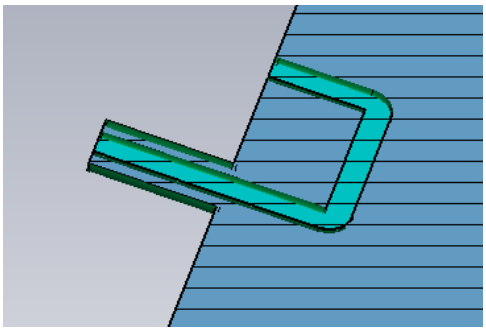

Fig. 8. Cross-Section of Input Coupler

In order to gain the highest efficiency in the cavity, the β of the input couplers added together should equal the β of the output coupler [5]. In order to do this, CST Microwave Studio is again used, using the Eigen Solver. In this mode, the Q-factor of the cavity can be calucated, as well as the

Q_{ext} of the couplers. Therefore, when the cavity is simulated with the output coupler alone, and with the input couplers alone, the β in each case should be equal.

The most interesting properties of this simulation cannot be determined using the Eigen Solver, and therefore the Frequency Domain solver must be used to find results such as S-parameters and field strength. The accuracy of the β calculations can be verified in this mode by finding the S-parameters at the input couplers. The reflection coefficient at each port will obey the equation, where N is the number of input couplers:

$$\Gamma = \frac{1-N}{N} \tag{17}$$

VIII. Output Coupler Design

The output coupler has the greatest flexibility in design. The basic design would start with a simple coaxial waveguide that extends into the cavity, with a matching β, using the Eigen Solver like the input coupler. In order to change the characteristics of the fields on the output coupler, various plates can be placed on the cavity end. As wells just having the inner conductor terminate in space in the cavity, it could terminate into a square plate or a cylindrical plate. The different sizes of these plates, as well as the length in the cavity can change the efficiency, β, and field characteristics of the coupler.

Once the power is fed through the coupler, in order to be fed into a larger system, a rectangular waveguide is often used. Therefore, a final design parameter would be the design of the coaxial to waveguide transistion. The coaxial line would usually terminate with in a T-junction that would finish at the walls of the waveguide. However, several designs do exist, and the best for the specific application would have to be utilized.

IX. Cavity Combiner Simulation Results

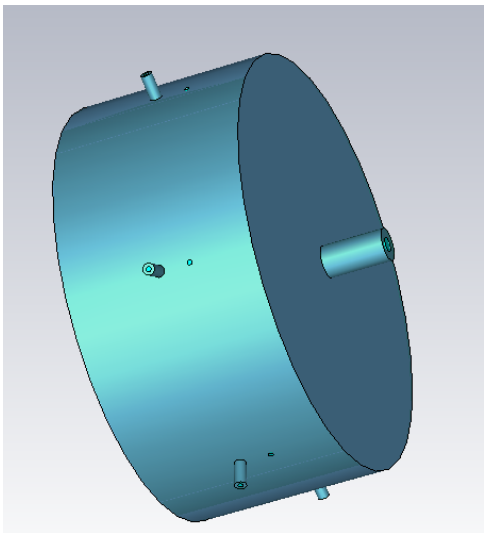

Fig. 9. Cavity Combiner

The results of the simulation agreed with the calculations presented above for the design of the cavity. The RF group at the Argonne Advanced Photon Source required a cavity design that would have six input couplers operating at 2 kW each, for a total of 12 kW. The biggest concerns were field breakdown and heating concerns. Any losses present in the simulation would create heat, and the design would have to make sure that this heating was not beyond the cooling capabilities present.

The easiest method of cooling would be either blowing air, or running water through pipes to cool the components. Therefore, if any losses are present, the easiest component to cool would be the cavity itself. If the output coupler is fed into a waveguide as in section VIII, then a cooling system is already in place for such transitions. This means the design could tolerate much higher losses on the output coupler if better results could be achieved this way. The losses on the input coupler were not much of a concern, since they are handling much less power than the output coupler. The power per input coupler is also decreased with additional ports, assuming the output power remains the same.

A. Plain Termination of Output Coupler

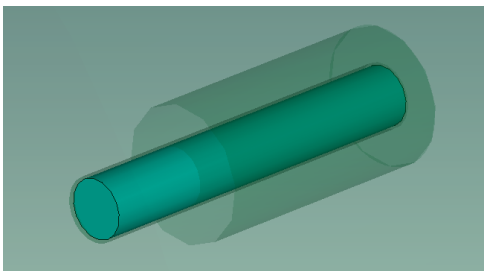

Fig. 10. Coaxial Termination of Output Coupler

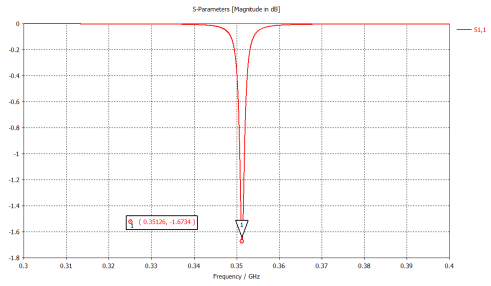

Fig. 11. Reflection at the Input Couplers for a Coaxial Output

The following table gives the losses present in selected surfaces when the output coupler is terminated in the cavity with no plate present. The input power is 500 mW total into the cavity.

As expected, the majority of the losses occured in the cavity. If the losses scale linearly, which is a reasonable assumption at these power levels, the output coupler losses are about 0.0185% of the input power. The losses present in the couplers, scaled to 12 kW total in the cavity, can

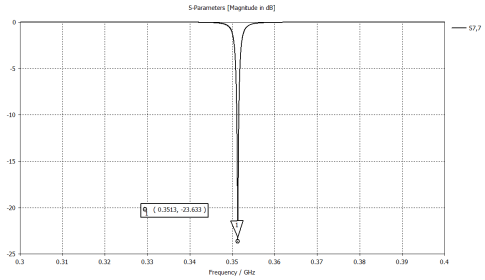

Fig. 12. Reflection at the Output Coupler for a Coaxial Termination

TABLE I
LOSSES IN CAVITY WITH NO PLATE.

Surface	Loss (μW)
Cavity	5047.2
Input Coupler	376.65
Output Coupler	92.553

reasonably be cooled. An eventual design goal is to match the specification of the ESRF cavity combiner, rated to handle 150 kW [2]. Even at those high power levels, if the losses still scale linearly, this coaxial design will have no problems being cooled. As seen in fig. 13, the losses along the output coupler were mostly evenly spread throughout the entire cable. The losses along the input coupler had build ups along the corners. This would mean that the input couplers would require more cooling, however since the power is spread out among all the couplers, this is not seen as a problem with the design.

The efficiency of the combiner is given in the following table:

TABLE II
EFFICIENCY OF CAVITY WITH NO PLATE.

Port	Power (mW)
Inputs	498.24
Output	487.55
Efficiency	97.51%

The input power at the ports being less than 500 mW occurs because of reflections. The port has a definite dip at the design frequency, but the reflection is still measured at about -26 dB, and so there will be minimal reflection.

As seen in figures 15 and 16, the poynting vectors are similar to the loss characteristics. There is no large build up of power on the output coupler. The input couplers do have some build up, but in order to get the correct fields inputted this would be challenging to correct. At the anticipated power levels, the input couplers should have no problems operating even with the build up. The output coupler will be water-cooled if needed, and therefore have high headroom if the design moves to higher power.

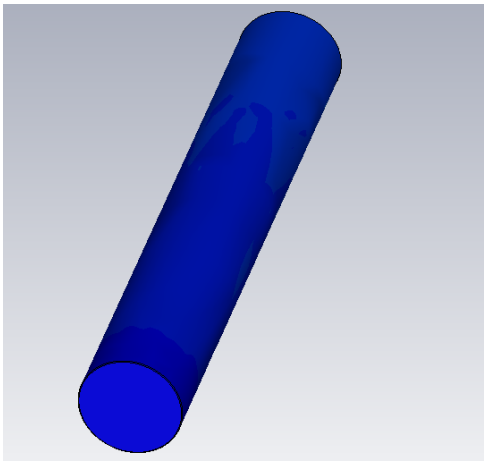

Fig. 13. Losses on the Coaxial Output Coupler

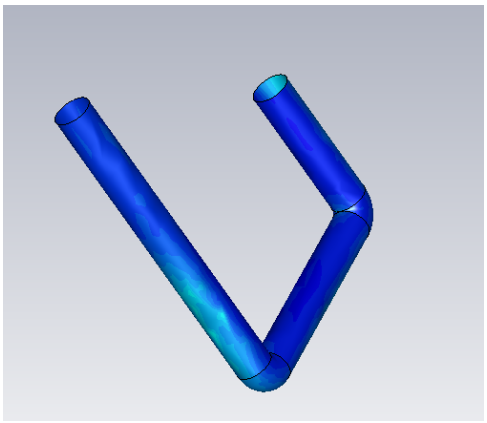

Fig. 14. Losses on the Coaxial Input Coupler

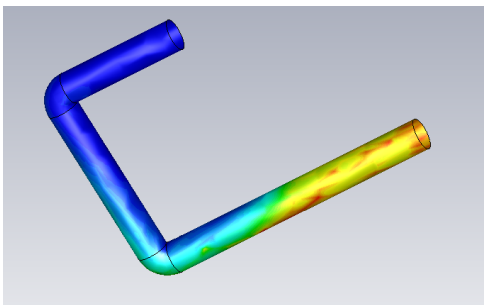

Fig. 15. Power Flow of the Coaxial Input Coupler

TABLE III
EFFICIENCY OF CAVITY WITH CYLINDRICAL PLATE.

Port	Power (mW)
Inputs	347.81
Output	344.628
Efficiency	68.925%

B. Cylindrical Plate Termination of Output Coupler

Placing a cylindrical plate on the end of the output coupler was also simulated, with the intention of reducing the build up of fields on the output coupler. With less fields, the need for

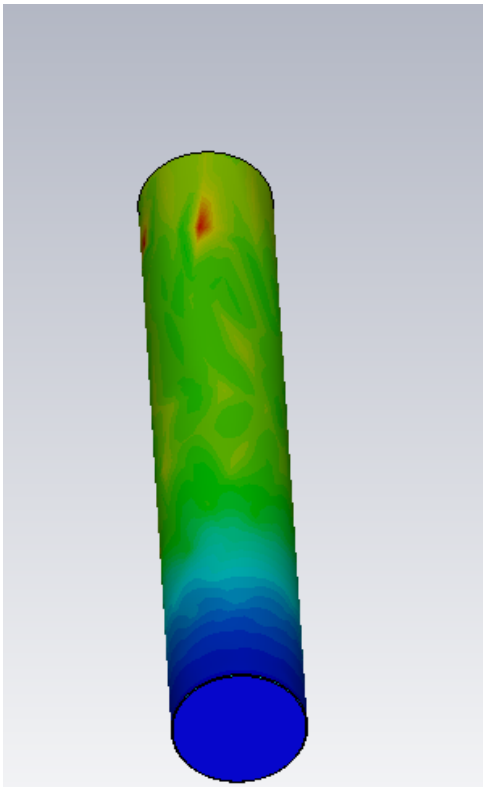

Fig. 16. Power Flow of the Coaxial Output Coupler

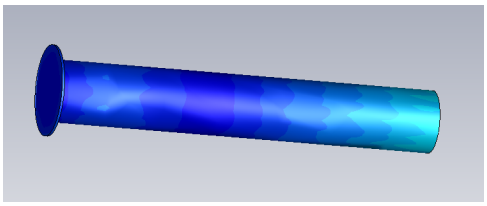

Fig. 17. Power Flow of the Cylindrical Output Coupler

cooling is reduced, and more power can be combined in the cavity. Unfortunately, matching the β of the output coupler with the cavity was not as simple as with the plain coaxial termination. The variables that influenced the β had much more interaction than with the simpler case. Therefore, in the final simulations performed, an efficiency of only 68% was achieved. This is obviously not acceptable, and more work needs to be done to manipulate the simulation and find parameters that give a useful efficiency level.

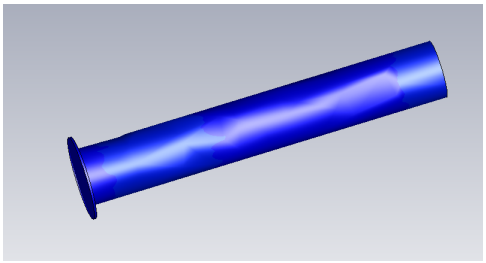

Fig. 18. Loss of the Cylindrical Output Coupler

TABLE IV
LOSSES IN CAVITY WITH CYLINDRTICAL PLATE.

Surface	Loss (μW)
Cavity	3058.85
Input Coupler	269.98
Output Coupler	36.8

If the low efficiency level is assumed to be reflected power at the input ports, and therefore the losses can be scaled, the cylindrical plate is a positive addition. The scaled losses on the input coupler remain about the same, but the losses on the output coupler are almost half. Obviously, these numbers need to be verified by a more accurate simulation that has an equivalent efficiency. However, with the results obtained, it is recommended that the cylindrical plate is worth investigating as a better output coupler.

X. CONCLUSION

The goal of this project was to simulate various power combiners, with the intention of eventually creating prototypes. The circuit simulation of the coaxial tree was a success, indicating the necessary sizes of various transformers needed. However, the 3D simulation of the coaxial tree did not agree with the circuit results. If the coaxial tree were to be constructed, the disparity would have to be rectified.
However, the prototype planned is the cavity combiner. Like the 3D simulation of the coaxial tree, the simulation of the cylindrical plate output coupler was not sucessful. The simulation of the coaxial output coupler agreed with the theoretical results, and the prototype could even begin construction using that design. If the cylindrical plate simulation is completed and shows much better results, then the prototype can be modified. With the current simulation, a prototype can be constructed with the given dimensions, and results similar to those given by the simulation is expected.

REFERENCES

[1] D. M. Pozar, *Microwave Engineering*, 3rd ed. New York, NY: Wiley, 2004.

[2] J. Jacob, "Rf solid state amplifiers," CERN Accelerator School on Power Converters, 2014.

[3] A. Danagoulian and G. Kohse. (2015) Resonant cavities and waveguides. [Online]. Available: http://web.mit.edu/22.09/ClassHandouts/Charged%20Particle%20Accel/CHAP12.PDF

[4] R. Kwok. (2015) Cavity resonators. [Online]. Available: http://www.engr.sjsu.edu/rkwow/EE172/Cavity_Resonator.pdf

[5] Y. Otake, J. Judkins, and H. Schwarz, "Cavity combiner for s-band solid-state amplifier for the high-power klystron at slac," 1990.